

이중유화 공정의 캡슐화 효율에 대한 모델링 연구

정영미[†] 

한국기술교육대학교 에너지신소재화학공학부
(2025년 3월 4일 접수, 2025년 7월 30일 수정, 2025년 9월 1일 채택)

Modeling of Encapsulation Efficiency for Double Emulsion Process

Young Mi Chung[†] 

Korea University of Technology and Education, School of Energy, Materials & Chemical Engineering,
Chungjeol-ro 1600, Cheonan 31253, Korea

(Received March 4, 2025; Revised July 30, 2025; Accepted September 1, 2025)

초록: 본 연구는 W1/O/W2 이중 유화(double emulsion) 방식을 활용한 미세캡슐화 공정에서 캡슐화 효율(EE, Encapsulation Efficiency)을 극대화하기 위한 공정 조건을 분석하였다. 분석 결과, 캡슐화 효율에 영향을 미치는 핵심 공정 변수로는 삼투압, 전단응력(shear stress), 그리고 역미셀(reverse micelles)의 유무가 포함됨을 확인하였다. 캡슐화 효율은 오일층(O)을 사이에 둔 삼투압 차($\Delta\Pi$)가 증가할수록 향상되지만, 특정 임계값을 초과하면 오히려 감소하였다. 또한, 역미셀을 도입할 경우 그렇지 않은 조건대비 캡슐화 효율이 현저히 개선되는 것으로 나타났다. 점도와 교반 속도 역시 중요한 역할을 하므로, 전단응력은 또 다른 핵심 요인이라 할 수 있다. 결국 EE의 최적화는 단일 공정 변수만으로 설명할 수 없으며, 모든 공정 변수가 복합적으로 EE에 영향을 미치는 것으로 밝혀졌다. 이에 본 연구에서는 새로운 무차원 수인 ‘캡슐화 수(Capsulation number, Cap)’를 제안하였으며, 최대의 EE를 달성하기 위해서는 Cap 이 약 300에 도달해야 하고, 동시에 $0.2 \text{ atm} < \Delta\Pi < 0.3 \text{ atm}$ 조건을 만족해야 함을 규명하였다.

Abstract: This study analyzes the process conditions for maximizing encapsulation efficiency (EE) in the microencapsulation process using the W1/O/W2 double emulsion method. The analysis results indicate that key process variables influencing encapsulation efficiency include osmotic pressure, shear stress, and the presence of reverse micelles. Encapsulation efficiency increases with $\Delta\Pi$, the osmotic pressure difference across the oil layer, but decreases after reaching a certain threshold. Additionally, the introduction of reverse micelles significantly improves encapsulation efficiency compared to the absence of reverse micelles. Since viscosity and mixing speed also play an important role, shear stress is another crucial factor. Optimization of EE cannot be explained by a single process variable alone, as all those process variables collectively influence EE. This study proposes a novel dimensionless number, named “Capsulation number (Cap)”. To achieve maximum EE, the Cap should reach approximately 300, while satisfying the condition of $0.2 \text{ atm} < \Delta\Pi < 0.3 \text{ atm}$.


Keywords: encapsulation efficiency, osmotic pressure, reverse micelle, capsulation number.

Introduction

The encapsulation technology using polymers has been advancing to ensure the stability of various substances and to create forms suitable for industrial applications. Encapsulation technology involves wrapping substances in various states with a thin polymer membrane, forming microparticles on the scale of a few micrometers.¹ When encapsulating drugs with biode-

gradable polymers, adjusting the polymer's shape, size, and properties can control the degradation time of the microparticles, thereby regulating the drug release rate.² This not only prevents the degradation of substances due to temperature, humidity, or microorganisms but also helps maintain therapeutic concentrations in the body, protects against rapid drug release, and allows injectable drugs to be converted into oral or mucosal formulations, reducing dosing frequency and side effects.^{2,4} Encapsulation technology is widely utilized in various fields, including pharmaceuticals, cosmetics, medicine, agriculture, and food.¹

Since polylactic acid (PLA) is relatively hydrophobic in the body, it has low cell affinity and degrades slowly. As a result, it

[†]To whom correspondence should be addressed.
quebecoise@koreatech.ac.kr,  0000-0002-8110-7066
©2025 The Polymer Society of Korea. All rights reserved.

can remain in the body for an extended period and induce inflammatory reactions during the degradation process.^{5,6} In contrast, ascorbic acid (AA) minimizes inflammation by down-regulating the expression of various inflammatory-inducing substances in the body and enhances antimicrobial effects by activating phagocytosis.^{7,8} Therefore, adding AA before introducing PLA into the body can help minimize inflammation caused by PLA.⁶ Additionally, both lactic acid (produced by PLA degradation) and AA strongly stimulate collagen synthesis, making them useful in the synthesis of cartilage and skin collagen.⁹⁻¹¹

In the W/O/W microparticle process of the double emulsion method, several factors influence the process, including polymer characteristics such as polymer chain length and polymer concentration in organic solvents, the volume of the internal aqueous phase (W1) and the continuous phase (W2), the concentration of additives such as surfactants or salts in both phases, homogenization speed, and the molecular weight of substances in the internal aqueous phase.¹² Polymer hydrophilicity varies depending on the chain length and functional groups, which can develop pores on the particles, altering degradation and drug release rates.¹² The polyvinyl alcohol (PVA) concentration in the external aqueous phase does not affect the internal W/O phase but increases the stability of the W/O/W emulsion as the external PVA concentration rises.¹³ Because the solidification of the emulsion into microparticles occurs through solvent evaporation, the PVA concentration in the external phase can influence the final particle size.¹⁴

When a surfactant like PVA is added to the internal aqueous phase, surfactant molecules spontaneously assemble at the interface during the formation of the aqueous-organic membrane, forming reverse micelles.¹⁵ Reverse micelles are spherical aggregates that form spontaneously through self-assembly of surfactant molecules in nonpolar organic solvents, requiring neither high energy nor shear conditions. These micelles create a highly flowable interface and can contribute to the formation of uniform particles, making them useful in microparticle production.¹⁶ Therefore, the reverse micelles formed by adding PVA to the internal aqueous phase prevent droplet coalescence, stabilizing the primary W/O emulsion and enhancing encapsulation efficiency.^{13,17} Shim *et al.* discussed the effect of process variables on microparticle size and yield, suggesting that the particle size remains nearly constant below a Reynolds number of 22000, above which droplet coalescence tends to occur.¹⁸

Combining ionic salts with AA can increase its stability by forming derivatives that convert to L-ascorbic acid through enzy-

matic reactions in the body.¹⁹ Additionally, adding salts to the aqueous phase helps prevent damage to the double-layered structure by reducing the risk of water penetration from the external phase into the internal phase due to osmotic pressure differences.²⁰ Studies have shown that adding salts in the microparticle process significantly influences osmotic pressure, interfacial tension, and reverse micelle formation, making it an important factor in microparticle production.²¹⁻²³ Yun and Chung discussed the influence of osmotic pressure on the encapsulation efficiency (EE) values and specifically demonstrated that the presence of salt in the internal W1 disrupts the particulate structure.²⁴

There have been efforts to optimize and standardize the double emulsion processes. Maa and Hsu explained the formation of microspheres by a liquid drop fragmentation mechanism using hydrodynamic model.²⁵ Zhou *et al.* attempted to explain EE by the Sauter mean diameter of primary emulsion using several key dimensionless numbers including Reynolds number and Weber number.²⁶ Yun and Chung explained droplet yield using the Capillary number and suggested that the EE value would be governed by thermodynamic equilibrium.²⁴ However, no model has been proposed to quantitatively implement osmotic pressure. Most model has been focusing on dynamics parameters rather thermodynamic parameters. There is a report that proposed a thermodynamic model by studying the effect of interaction energy between each interface on the EE.²⁷ However, since EE is a result of the complex interplay of various process variables, it cannot be simply interpreted based on dynamic or thermodynamic factors alone. This is because all variables influence the EE value simultaneously. The encapsulation process is a combination of multiple factors. Currently, no model includes the presence of reverse micelles.

In this study, biodegradable polymer PLA was used to produce microparticles through a W/O/W double emulsion process to protect AA from degradation. The goal was to identify process conditions that maximize the EE value. The effects of key process variables on EE of AA were analyzed, and a universal model integrating these process variables was proposed. The model proposed in this study encompasses both dynamic and thermodynamic aspects, and incorporates various process variables, including the presence or absence of reverse micelles.

Experimental

Reagents and Materials. Two types of natural polymer PLA (Poly(L-lactic acid)) were used to prepare the microparticles. PLA with MI = 3 g/10 min (measured at 190 °C/2.16 kg) was

purchased from LX575 (Total-Corbion, Netherlands), while PLA with MI = 30 g/10 min was purchased from FY201 (Dreamy Co., Korea). Since the molecular weight data of PLA was not provided by the manufacturers, we designate the low-viscosity, high-flowability FY201 as LPLA and the high-viscosity, low-flowability LX575 as HPLA for convenience. PLA was dissolved in dichloromethane (DCM, SAMCHUN, 99.5%, Extra pure, Korea) to prepare the organic phase. Polyvinyl alcohol (PVA, 1500, CP grade, Daejung Chemicals, Korea) was used as a surfactant. L(+)-Ascorbic acid (Daejung Chemicals & Metals co., LTD, 99%, EP, Korea) was incorporated into the microparticles, while sodium chloride (Daejung Chemicals & Metals co., LTD, 99%, EP, Korea) was used as a salt, both obtained from Daejung Chemicals. The reagents for the HPLC mobile phase were NaH_2PO_4 (99%, EP, Daejung Chemicals, Korea) and ethanol ($\text{C}_2\text{H}_5\text{OH}$, 95% EP, Dusan Pharmaceutical, Korea).

Microcapsule Preparation. PLA was weighed to achieve concentrations of 2, 6, 10 wt% and dissolved completely in DCM. PVA was weighed to 1 wt% of the total mass and dissolved in distilled water. To prepare the aqueous phase for encapsulation, AA was dissolved in distilled water at 20 wt% and stirred at room temperature under light shielding. The solution was freshly prepared before sample preparation. The solutions were accurately weighed and mixed at 225 rps (round per second) using a homogenizer (DAIHAN, HG-15A-set A, Korea). The process including reverse micelle formation was carried out sequentially as described by Yun and Chung.²³ For conditions involving salt, NaCl was added to W1 and W2 at concentrations ranging from 0~1 wt% for W1 and 0~6% for W2. The resulting W1/O/W2 dispersion was processed by removing the organic solvent and drying the precipitated microparticles. DCM was evaporated using a rotary evaporator (Scilab, EV-1001V, Korea) at 40 °C for 2 hours at 5 rpm. The precipitated microparticles were transferred to a beaker and washed with distilled water. To remove residual organic solvent and surfactant, centrifugation (Nasco Korea, DT5-2B, Korea) was performed, followed by vortexing and redistribution into 50 mL tubes. This process was repeated twice. The washed particles were dried using a freeze dryer (OPERON ADVANTECH, LYB-8604, Korea). The final dried microparticles were weighed to determine yield and used for HPLC analysis. The yield of microparticles was calculated using the following equation:

$$\text{Yield (\%)} = \frac{\text{Mass of particles produced}}{\text{Mass of initial polymer material} + \text{AA}} \times 100 (\%) \quad (1)$$

Encapsulation Analysis. For encapsulation efficiency (EE) analysis, 50 mg of microparticles were aliquoted into Eppen-

dorf tubes (E-tubes). Each E-tube was filled with 1 mL of distilled water, vortexed, and centrifuged to remove the supernatant. This washing process was repeated four times to remove residual AA on the particle surface, ensuring only encapsulated AA was measured. After washing, 0.3 mL of DCM was added to each centrifuge tube to dissolve the PLA, followed by 1 mL of 5% metaphosphoric acid (GR, Kanto Chemical, Japan) to prevent AA degradation. The mixture was vortexed to allow AA to be extracted into the aqueous layer. After centrifugation, the organic and aqueous phases were separated. The aqueous phase was filtered through a 0.2 μm PTFE-H syringe filter, and AA content was analyzed by HPLC (HITACHI Primaide PM1000 Series, Hitachi, Japan) at a wavelength of 265 nm. The HPLC analysis used a Quasar SPP C18 column (250 mm \times 4.6 mm, 0.5 μm , Perkin Elmer, N9308955, USA) with a mobile phase of 2.5% ethanol + 25 mmol/L NaH_2PO_4 (pH 4.7) at a flow rate of 0.5 mL/min. The encapsulation efficiency was calculated using the following equation:

$$\text{EE (\%)} = \frac{\text{Mass of AA in nanoparticles}}{\text{Mass of AA in formulation}} \times 100 (\%) \quad (2)$$

Before conducting the EE analysis, a preliminary study was carried out to investigate the degradation of AA due to the heat generated by the homogenizer. A comparative experiment was conducted by mixing only the AA aqueous solution with the homogenizer. Even after operating the homogenizer at its maximum allowable limit (400 rps), no decrease in AA concentration was observed. Therefore, one can conclude that the EE values obtained from this work is purely from the AA concentration encapsulated inside the microcapsules.

The shape, size, and surface morphology of the microparticles were observed using a scanning electron microscope (SEM, JEOL-6510, Japan) at 500 \times magnification. Each sample was tested at least twice to ensure reproducibility, and the average values were calculated.

Process Parameter Measurement. The viscosity of the prepared solutions was analyzed to examine its effect on microparticle formation. The in-situ viscometer and measurement followed the method of Yun and Chung.²³ To assess the interfacial tension between the W1 and O phases during the initial droplet formation, a contact angle analyzer (SEO, DCA-200, Korea) was used. The interfacial tension values for W1 (σ_1) and W2 (σ_2) were measured under the same sample compositions as in the experiment. To quantify the effect of osmotic pressure on microparticles, the osmotic pressure of the internal and external aqueous phases was calculated for each condition. The den-

sity values used for these calculations were obtained using a density measurement jig attached to the interfacial tension analyzer. The osmotic pressure was calculated using equations (3), (7), (8), while the van 't Hoff factor i for AA was determined from pH values measured using a pH meter (HORIBA, LAQUA F-71) and calculated using equations (4)–(6). The i values for AA were measured to be close to 1, indicating that changes in i due to AA dissociation are negligible.

$$\Pi = iCRT \quad (3)$$



$$[H^+] = [A^-] = a \quad (5)$$

$$[HA] = [HA]_i - a \quad (6)$$

$$i = \frac{[H^+] + [A^-] + [HA]}{[HA]_i} = \frac{a + a + [HA]_i - a}{[HA]_i} = 1 + \frac{a}{[HA]_i} \quad (7)$$

$$\Pi_{\text{total}} = \Pi_{\text{AA}} + \Pi_{\text{NaCl}} + \Pi_{\text{PVA}} \quad (8)$$

In the above equation, Π represents osmotic pressure (atm), i is the van 't Hoff factor, C is the molar concentration of the solute (mol/L), R is the gas constant (0.0821 atm·L/mol·K), and T is the absolute temperature (K). The $[HA]_i$ values in equations (6) and (7) represent the molar concentration of AA solution (mol/L). In equations (8), the contribution of PVA to osmotic pressure was almost negligible. According to William *et al.*,²⁸ the i value of NaCl can be approximated to be 2 below the concentration of 1 molality, which corresponds to about 6% (w/w) for NaCl. Therefore, i value of 2 was adopted to calculate Π_{NaCl} as the concentration of NaCl upto 6% was adopted in this study.

Results and Discussion

Influence of Process Variables. Figure 1 illustrates the changes in the EE of LPLA and HPLA microcapsules as the salt concentration in W2 increases. The legends in Figure 1(a) are displayed at the top left of the graph. The label "AA10%/LPLA10%/salt 0–6%," for example, indicates the composition of the W1/O/W2 system in sequential order. AA10% means the percentage of AA in W1 phase and the "10%" in LPLA10% refers to the mass percentage of LPLA in the oil phase. Lastly, salt 0–6% indicates the NaCl % in W2 phase. If reverse micelles were introduced into W1, RM is attached after AA percentage such as "AA10%RM". All samples in Figure 1(a) to (f) have 0% additional salt in W1, meaning that the primary factor causing osmotic pressure in W1 is the encapsulated AA inside the microcapsules.

Figure 1(a) and (b) compare cases with and without the application of reverse micelles for the same composition. It is clearly observed that applying reverse micelles (b) leads to an increase in EE values. Additionally, increasing the salt concentration in the W2 phase further enhances the EE value. An interesting observation in (b) is that while EE values initially rise with increasing $\Delta\Pi$ (W2-W1), they start to decrease when osmotic pressure difference $\Delta\Pi$ reaches about 0.2. This is likely because, beyond a certain threshold, ample amount of water in W1 migrates to W2, causing the microparticle structure to start shrinking and collapsing.

This tendency becomes more pronounced with the introduction of reverse micelles, which appear to stabilize the W1/O/W2 structure by enabling it to withstand osmotic pressure differences ($\Delta\Pi$) of less than approximately 0.2. However, beyond this threshold, the structure seems to collapse. It is presumed that the reverse micelles help maintain the integrity of the organic phase surrounding the inner aqueous phase at the W1/O interface, thereby preventing structural disintegration and protecting the microparticles from damage even under conditions where an osmotic gradient exists.

Figure 1(c) represents a case where the AA concentration is reduced to half compared to (b), thereby lowering the osmotic pressure in W1. As observed in Figure 1(b), the same pattern is seen in (c), where increasing $\Delta\Pi$ leads to higher EE values. However, unlike (b), where EE values decrease from $\Delta\Pi$ of 0.28, in (c), the decline in EE is observed from approximately 0.18. This suggests that in (c), the osmotic pressure within W1 is lower than in (b), making it unable to withstand high W2 salt concentrations, leading to an earlier structural collapse. Figures 1(a) to (c) and Figures 1(d) to (f) compare LPLA and HPLA, representing low-molecular-weight and high-molecular-weight PLA, respectively. The results show that using HPLA results in higher EE values. Furthermore, within the same graph, increasing the concentration of LPLA or HPLA also leads to higher EE values. This is attributed to higher viscosity of oil phase resulting in more robust oil layer, preventing the collapse of overall W1/O/W2 structure.

Intuitively, the W1/O/W2 structure is expected to be most stable when $\Delta\Pi$ approaches zero. However, in reality, the highest EE values are observed in the range of 0.2 atm < $\Delta\Pi$ < 0.3 atm. This suggests that for higher encapsulation efficiency, the osmotic pressure of W2 must be slightly greater than that of W1.

From these results, it can be inferred that the key process variables influencing EE values include:

- (1) The introduction of reverse micelles in W1

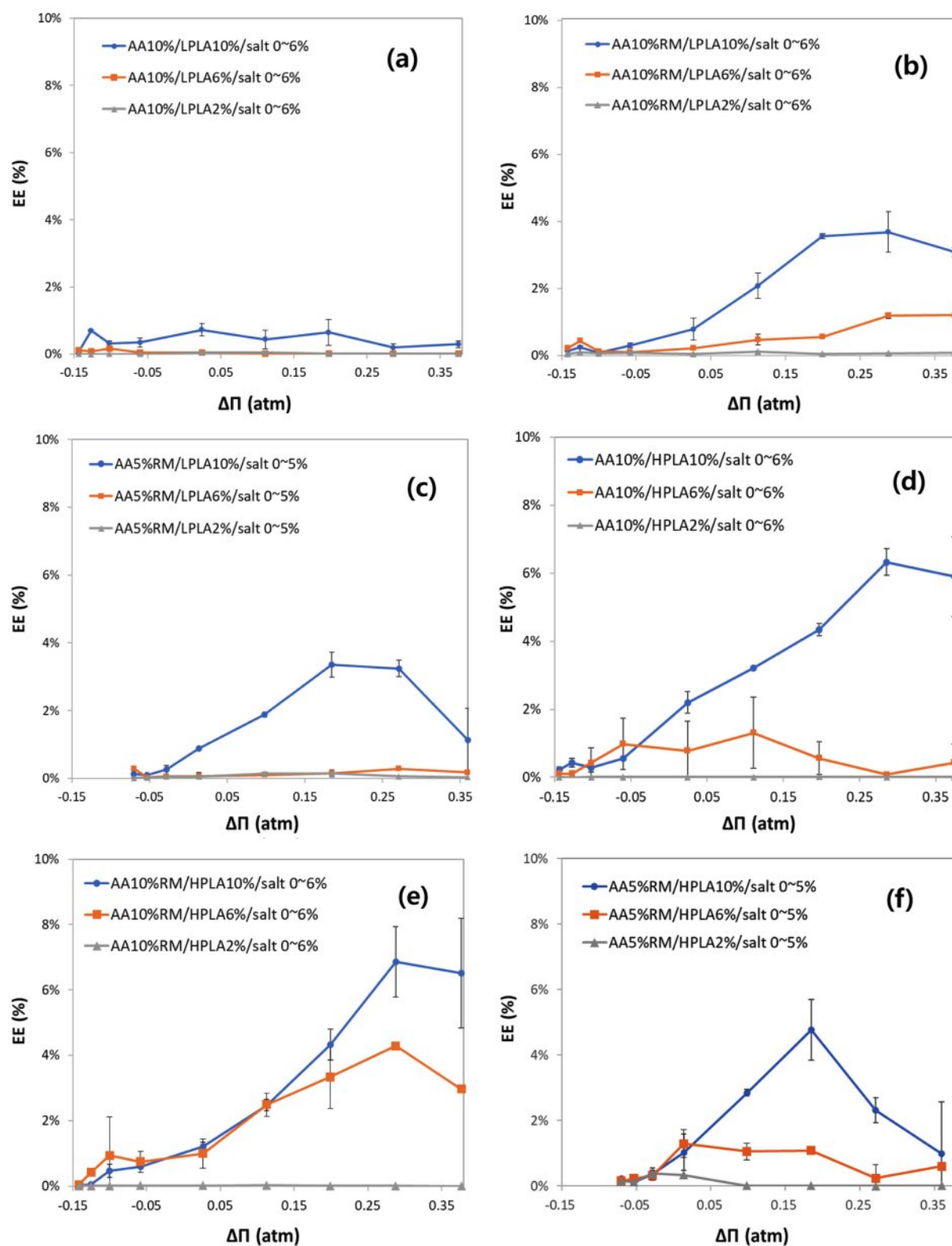


Figure 1. EE values at varying $\Delta\Pi$ (W2-W1): (a) at no reverse micelle using LPLA; (b) with reverse micelle and high AA concentration in W1 using LPLA; (c) with reverse micelle condition and low AA concentration in W1 using LPLA; (d) at no reverse micelle using HPLA; (e) with reverse micelle and high AA concentration in W1 using HPLA; (f) with reverse micelle and low AA concentration in W1 using HPLA.

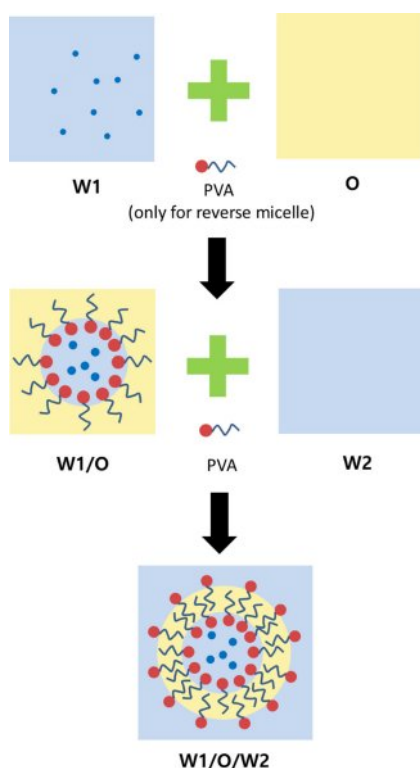


Figure 2. Schematic diagram of reverse micelle formation.

- (2) The osmotic pressure difference between W2 and W1
- (3) The viscosity of the oil phase

So far, these factors seem to play a crucial role in determining EE values and maintaining the structural stability of the micro-particles. Regarding first factor above, the contribution of reverse micelles to the structural stability of the microparticles can be explained as shown in the schematic diagram, Figure 2.

Regarding the second factor, water layers W1 and W2, separated by an oil layer, exert osmotic pressure against the oil layer. The direction of water movement is expected to depend on the difference between these two values. Before the particles solidify, in their droplet state, the oil layer exists as a very thin and unstable membrane. In such a state, it is believed that water from the inner (W1) and outer (W2) phases can permeate through the oil layer depending on the osmotic conditions.

Contrary to the expectation that droplets would be most stable when $\Delta\Pi = 0$, in Figure 1, the highest encapsulation efficiency (EE) was observed at slightly positive values of $\Delta\Pi$. In the case of $\Delta\Pi < 0$, EE was significantly low. This suggests that when the osmotic pressure of W1 is higher than that of W2, water may permeate inward through the oil membrane, causing its rupture and resulting in structural instability of the droplets. On the other hand, when $\Delta\Pi > 0$, water tends to move from W1 to W2, which

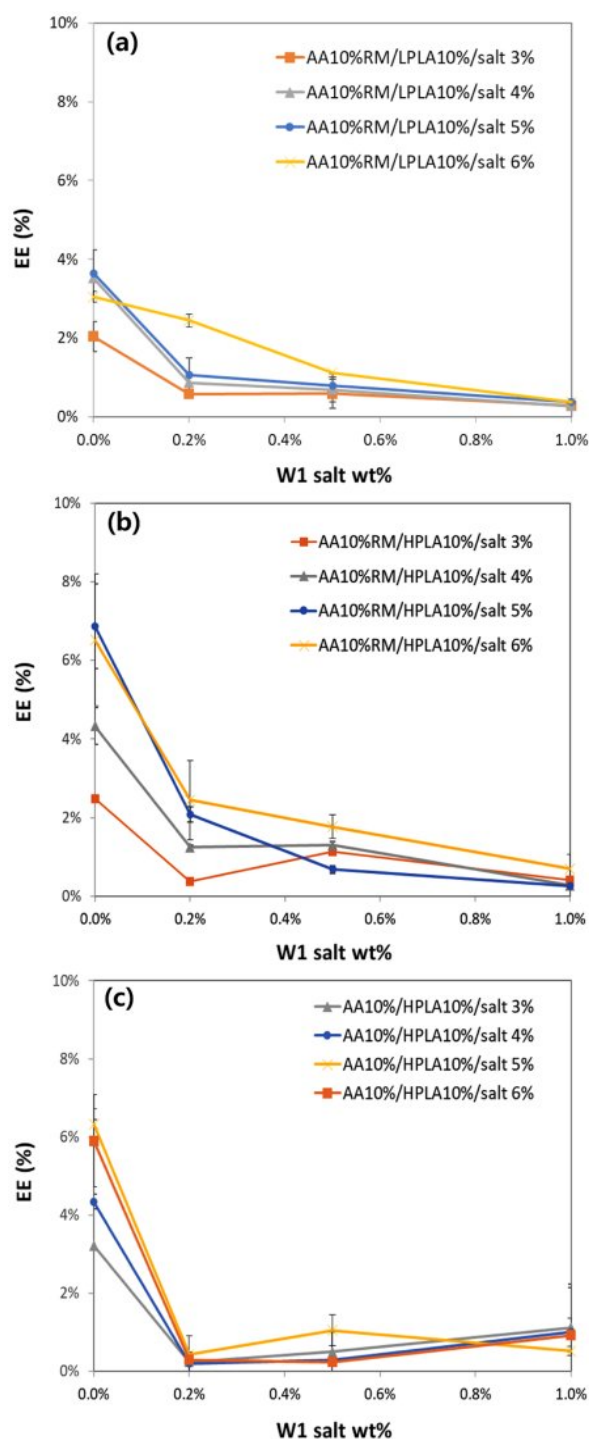


Figure 3. Effect of W1 salt concentration on EE: (a) at LPLA with reverse micelle; (b) HPLA with reverse micelle; (c) HPLA without reverse micelle.

could exert compressive pressure on the droplets, but does not appear to cause rupture. In fact, the high osmotic pressure of W2 may stabilize the droplet structure and offset the stretching capillary effect induced by surrounding shear forces. Also, as

mentioned earlier, the introduction of reverse micelles into the W1 phase is presumed to provide resistance against the strong osmotic pressure exerted by the outer aqueous phase (W2), thereby preventing structural collapse and protecting the microparticles from damage.

Figure 3 examines the changes in EE values due to the difference in salt concentration between W1 and W2. As shown in the graph, the EE value decreases sharply as the W1 salt concentration increases from 0% to 0.2%. This suggests that as the salt concentration in W1 rises, the collapse of the oil layer protecting the W1 aqueous phase accelerates. In the W1/O/W2 structure, W1, which is relatively small in volume and trapped within the oil layer, seems highly sensitive to osmotic pressure. When the internal osmotic pressure of W1 increases, water influx from the external aqueous phase (W2) occurs, causing the relatively small microdroplets to expand rapidly, ultimately leading to structural failure.

Figure 4 illustrates the effect of rotational speed on the formation of microdroplets during mixing with a homogenizer. The rotational speed in rps (rounds per second) was tested at three points: 180, 225, and 270 rps. At speeds below 180 rps, dispersion was insufficient due to low shear force, while at speeds above 270 rps, phase separation occurred. Therefore, experiments were conducted only under these three conditions. As shown in Figures 4, both LPLA and HPLA exhibited the highest EE values at the intermediate speed of 225 rps. This confirms that, in addition to thermodynamic factors such as osmotic pressure, dynamic factors also influence EE values. Furthermore, since

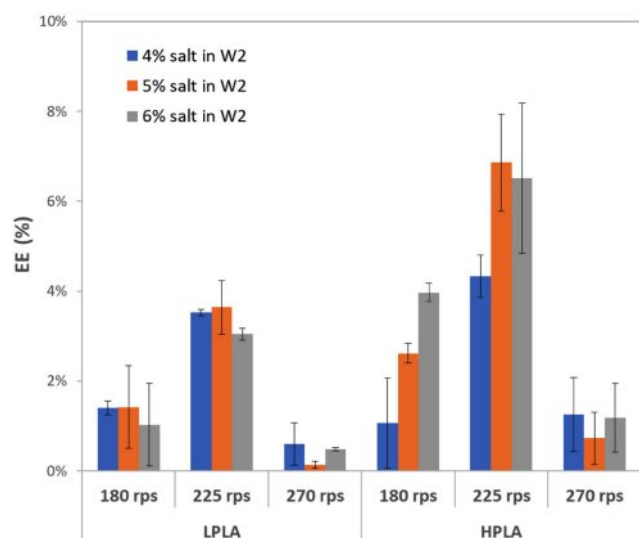


Figure 4. Effect of mixing rotational speed on EE at LPLA and HPLA.

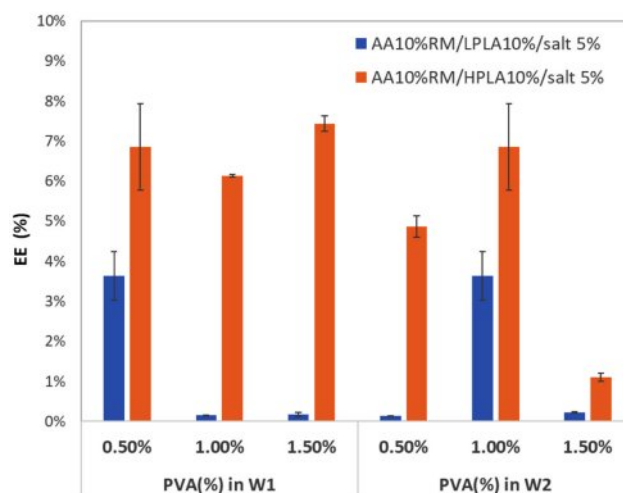


Figure 5. Effect of PVA concentration of W1 and W2 on EE.

EE values do not show a consistent increasing or decreasing trend with rps, the introduction of additional variables is necessary for a more comprehensive explanation.

Figure 5 compares EE values based on the PVA content used as a surfactant. Comparisons were made at PVA concentrations of 0.5~1.5% in W1 and W2 as microdroplet formation was not well achieved outside this range. As can be seen from the EE variation for PVA in W1, LPLA and HPLA exhibit different behaviors. In the case of LPLA, an increase in PVA content leads to a sharp decline in encapsulation efficiency, whereas for HPLA, EE remains stable or even increases. On the other hand, PVA changes in W2 exhibit different tendency from PVA changes in W1. PVA of 1% in W2 gives the best EE. As seen in Figure 4, Figure 5 also does not exhibit a consistent trend. Therefore, EE is assumed to be influenced by a complex interplay of multiple variables, which justifies the need to develop a universal model that integrates all these factors.

Modeling. As discussed in the previous section, the encapsulation efficiency (EE) is significantly affected by process variables including the osmotic pressure difference ($\Delta\Pi = W_2 - W_1$), viscosity, mixing speed, and interfacial tension. Figure 6 visualizes these process variables and their effects around the W1/O/W2 microdroplets. Here, lateral pressure is equivalent to the shear stress applied to the oil phase. According to the preliminary study by Yun and Chung,²³ the droplets elongate and break up due to capillary action during the formation of W1/O/W2 droplets. Based on this theory, they demonstrated that the Capillary number (Ca), a dimensionless parameter combining the Reynolds number (Re) and the Weber number (We), is a critical factor in the droplet formation process. Among the key physical

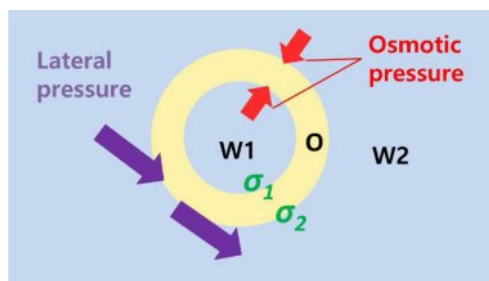


Figure 6. Schematic diagram of process variables affecting EE.

properties involved in calculating the capillary number, interfacial tension plays an important role.

The presence or absence of reverse micelles affects the interfacial tension, which ultimately influences the interfacial tension ratio (σ_1/σ_2) shown in Figure 6. This interfacial tension ratio is a dimensionless number that seemingly determines the curvature of the oil film and can be defined as a *curvature factor*, one of the shape factors. In other words, it can be considered a key thermodynamic variable in maintaining the shape of the droplet.

The capillary action is directly related to the lateral pressure in Figure 6. Therefore, one can expect that the lateral pressure is an important factor for the formation of droplets. For the case of *EE*, as shown in Figure 6, osmotic pressure affects the oil layer in the perpendicular direction, while shear stress influences it in the tangential direction, ultimately impacting the *EE* value. Such lateral pressure (shear stress) and normal pressure (osmotic pressure) should be balanced with each other. Maintaining this balance is crucial for preventing the droplet from becoming deformed to one side. This ensures that the spherical structure remains stable, making it an important factor during a W1/O/W2 droplet formation. The ratio of the two pressures can be expressed as a dimensionless number, i.e. $\Delta\Pi/(\mu \cdot n)$, which is defined as *sphericity factor* in this work.

Note that the term *sphericity factor* does not necessarily refer to the actual shape of the droplet, but rather implies the recovery time after the droplet has been more deformed along one axis due to excessive stress. For example, when the difference between the two stress values deviates from the optimal point, the recovery time to a spherical shape should increase.

To integrate all these process variables, a universal model is proposed in the form of a dimensionless number, which we define as the *Capsulation number*, or *Cap*. This dimensionless number is formulated based on the ratio of two pressures and interfacial tensions.

$$Cap = \text{sphericity} \cdot \text{curvature} = \left(\frac{\Delta\Pi}{\mu \cdot n} \right) \left(\frac{\sigma_1}{\sigma_2} \right) \quad (9)$$

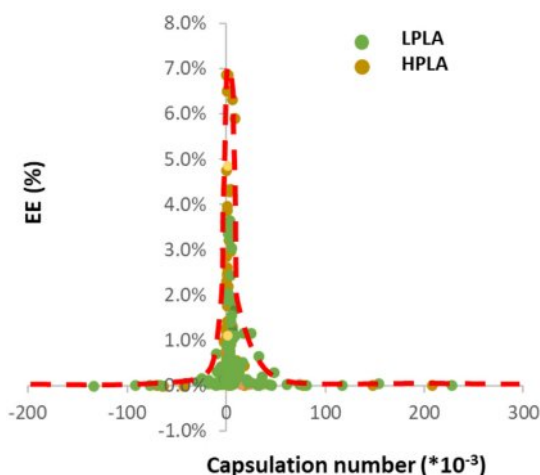


Figure 7. Plot of EE vs. Capsulation number.

μ = viscosity of the fluid

n = rotational speed (s^{-1})

$\Delta\Pi$ = osmotic pressure difference across the sphere

σ_1 = Interfacial tension between W1/O phases

σ_2 = Interfacial tension between O/W2 phases

Equation (9) consists of osmotic pressure to lateral pressure ratio and interfacial tension ratio. The interfacial tension ratio is closely related to the presence of reverse micelles. Introducing reverse micelles significantly reduces the W1/O interfacial tension, thereby also decreasing the interfacial tension ratio in equation (9).

When *EE* values are plotted as a function of this dimensionless number, the resulting graph follows a delta function pattern, similar to Figure 7. In Figure 7, *EE* reaches its peak near $Cap = 300$. However, all the conditions satisfying $Cap \sim 300$ do not necessarily give maximum *EE*. As explained in Figure 2, optimal conditions for achieving a high *EE* value must fall within the range of $0.2 \text{ atm} < \Delta\Pi < 0.3 \text{ atm}$. Therefore, both $Cap \sim 300$ and $0.2 \text{ atm} < \Delta\Pi < 0.3 \text{ atm}$ should lead to maximum *EE*.

Among the variables that make up the *Cap* number, osmotic pressure is approximately 1000 times greater than shear stress. This indicates that the intensity of osmotic pressure around the droplet overwhelmingly dominates shear stress, making osmotic pressure—the thermodynamic factor—a more decisive element in determining the *EE* value. However, since the dynamics of droplet formation also have a significant influence, this factor cannot be overlooked in modeling as proved in Figure 4. In Figure 7, the x-axis represents the *Cap* value divided by 1000 to avoid large numerical notation.

Morphology. Figure 8 compares SEM images of micropar-

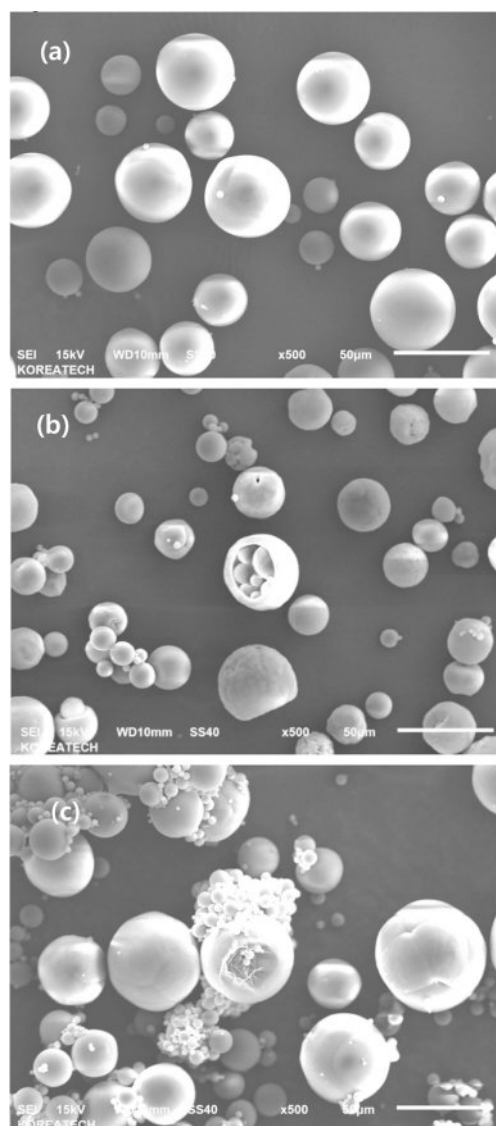


Figure 8. SEM images of microparticles produced at (a) $Cap = 236$ at $\Delta\Pi = 0.28$ (b) $Cap = -630$; (c) $Cap = 14500$.

ticles produced under various process conditions corresponding to diverse Cap numbers of -630, 240 and 14500. As seen in Figure 8(a), microparticles produced under optimal condition close to $Cap \sim 300$ exhibit robust and stable structure. On the other hand, microparticles produced under far extreme conditions on both ends, i.e. -630 (Figure 8(b)) and 14500 (Figure 8(c)) exhibit deformed and even ruptured structure. These three conditions showed similar yield values because the obtained particles exhibited similar mass values regardless of whether they ruptured or not. As mentioned above, the formation of microparticles is determined mostly by dynamics such as shear stress but it is not the main factor to affect EE. This demonstrates that desired EE can only be expected by employing optimized pro-

cess conditions, combination of Cap and $\Delta\Pi$.

Conclusions

This study defines the process variables for maximizing the EE value in the microparticle manufacturing process using W1/O/W2 double emulsion and quantitatively analyzes and compares their effects. First, it was found that the difference in osmotic pressure acting inside and outside the oil layer is a crucial factor in encapsulating the water-soluble component, Ascorbic acid. Additionally, the introduction of reverse micelles was identified as another key variable. Furthermore, it was discovered that mixing speed during homogenization and the viscosity of the oil phase are also important process variables influencing the EE value. In quantifying these effects, it was observed that osmotic pressure and shear stress competitively influence droplets formation and EE, while reverse micelles directly affect interfacial tension. Therefore, the ratio of interfacial tensions (W1/O and O/W2) is a critical factor in determining the EE value.

By integrating all these process variables, a novel dimensionless number was developed, named as Capsulation number (Cap). The EE vs. Cap relationship exhibits a pattern similar to a delta function, peaking around $Cap = 300$. However, achieving a high EE value is not guaranteed under all conditions near $Cap \sim 300$; the additional condition of $0.2 < \Delta\Pi < 0.3$ must also be satisfied. SEM imaging of actual samples confirmed that microparticles meeting both conditions exhibit a robust structure, whereas samples with conditions deviating far from the optimal condition, for example $Cap \sim -600$, display unstable and ruptured microparticles.

This new dimensionless number will serve as an important guideline for process optimization. Instead of testing various process variables individually to find the optimal conditions for the highest EE value, we recommend implementing the process based on the Cap optimum point presented in this study. This approach is also highly useful for process scale-up, as the dimensionless number remains consistent regardless of scale. In other words, there is no need for costly process optimization experiments when transitioning from lab scale to mass production. Ultimately, this eliminates the need for endless trial-and-error approaches, making it highly practical for real-world applications in fields such as cosmetics and pharmaceuticals where encapsulation processes are used.

Acknowledgments: This research was supported by “Regional Innovation Strategy (RIS)” through the National Research Foundation of Korea (NRF) funded by the Ministry of Edu-

cation (MOE) (2021RIS-004) and the Education and Research Promotion Program of KOREATECH in 2024.

Conflict of Interest: The authors declare that there is no conflict of interest.

References

- Silva, P. T.; Fries, L. L. M.; de Menezes, C. R.; Holkem, A. T.; Schwan, C. L.; Wigmann, É. F.; Bastos, J. O.; Silva, C. B. Microencapsulation: Concepts, Mechanisms, Methods and Some Applications in Food Technology. *Cienc. Rural.* **2014**, 44, 1304-1311.
- Ma, G. Microencapsulation of Protein Drugs for Drug Delivery: Strategy, Preparation, and Applications. *J. Control. Release* **2014**, 193, 324-340.
- Yu, J. H.; Jung, I. I.; Lee, J. E.; Lim, G. B. Preparation of Gemcitabine-Loaded Methoxy Poly(ethylene glycol)-*b*-Poly(*L*-lactide) Microparticles Using W/O/W Multiple Emulsion Method, *KSBB J.* **2011**, 26, 333-340.
- Hong, J. H.; Song, K. S.; Kim, K. J.; Lee, C. S.; Ahn, B. M.; and Kim, B. S. Nano-capsulation of *L*-Ascorbic Acid in Nonaqueous System. *J. Korean Ind. Eng. Chem.* **2008**, 19, 604-608.
- Rasal, R. M.; Janorkar, A. V.; Hirt, D. E. Poly (lactic acid) Modifications. *Prog. Polym. Sci.* **2010**, 35, 338-356.
- Popelka, A.; Abdulkareem, A.; Mahmoud, A. A.; Nassr, M. G.; Mohamoud, M. K. A. A.; Mohamoud, K. J.; Hussein, M. K.; Lehoc, M.; Vesela, D.; Humpolíček, P.; Kasak, P. Antimicrobial Modification of PLA Scaffolds with Ascorbic and Fumaric Acids via Plasma Treatment. *Surf. Coat. Technol.* **2020**, 400, 126216.
- Carr, A.; Maggini, S. Vitamin C and Immune Function. *Nutrients* **2017**, 9, 1211.
- Gęgotek, A.; Skrzydlewska, E. Antioxidative and Anti-Inflammatory Activity of Ascorbic Acid. *Antioxidants* **2022**, 1993.
- Mangir, N.; Bullock, A. J.; Roman, S.; Osman, N.; Chapple, C.; MacNeil, S. Production of Ascorbic Acid Releasing Biomaterials for Pelvic Floor Repair. *Acta Biomater* **2016**, 29, 188-197.
- Jin, H. R. Generation of Human Cartilage Tissue Using Tissue Engineering. *Korean J. Otorhinolaryngol-Head Neck Surg.* **2003**, 46, 355-363.
- Fitzgerald, R.; Bass, L. M.; Goldberg, D. J.; Graivier, M. H.; Lorenc, Z. P. Physicochemical Characteristics of Poly-L-lactic Acid (PLLA). *Aesthet Surg J.* **2018**, 38, 13-17.
- Mao, S.; Xu, J.; Cai, C.; Germershaus, O.; Schaper, A.; Kissel, T. Effect of WOW Process Parameters on Morphology and Burst Release of FITC-Dextran Loaded PLGA Microspheres. *Int. J. Pharm.* **2007**, 334, 137-148.
- Yang, Y. Morphology, Drug Distribution, and In Vitro Release Profiles of Biodegradable Polymeric Microspheres Containing Protein Fabricated by Double-Emulsion Solvent Extraction/Evaporation Method. *Biomaterials* **2001**, 22, 231-241.
- Kim, H. K.; Park, T. G. Comparative Study on Sustained Release of Human Growth Hormone from Semi-Crystalline Poly(*L*-lactic acid) and Amorphous Poly(*D,L*-lactic-co-glycolic acid) Microspheres: Morphological Effect on Protein Release. *J. Control. Release* **2004**, 98, 115-125.
- Li, Z.; Liu, H.; Zeng, L.; Liu, H.; Yang, S.; Wang, Y. Preparation of High Internal Water-Phase Double Emulsions Stabilized by a Single Anionic Surfactant for Fabricating Interconnecting Porous Polymer Microspheres. *Langmuir* **2014**, 30, 12154-12163.
- Arsene, M.-L.; Răut, I.; Călin, M.; Jecu, M.-L.; Doni, M.; Gurban, A.-M. Versatility of Reverse Micelles: From Biomimetic Models to Nano (Bio)Sensor Design. *Processes* **2021**, 9, 345.
- Ohwaki, T.; Machida, R.; Ozawa, H.; Kawashima, Y.; Hino, T.; Takeuchi, H.; Niwa, T. Improvement of the Stability of Water-in-oil-in-water Multiple Emulsions by the Addition of Surfactants in the Internal Aqueous Phase of the Emulsions. *Int. J. Pharm.* **1993**, 93, 61-74.
- Shim, J.-R.; Hwang, J.-Y.; Park, J.-S.; Chung, Y. M. Process Optimization of PLA Microbead Production. *J. Korea Academia-Industrial.* **2022**, 23, 538-547.
- Caritá, A. C.; Fonseca-Santos, B.; Shultz, J. D.; Michniak-Kohn, B.; Chorilli, M.; Leonardi, G. R. Vitamin C: One Compound, Several Uses. Advances for Delivery, Efficiency and Stability. *Nanomedicine* **2020**, 24, 102117.
- Rosano, H. L.; Gandolfo, F. G.; Hidrot, J.-D. P. Stability of W1/O/W2 Multiple Emulsions. *Colloids Surf. A Physicochem. Eng. Asp.* **1998**, 138, 109-121.
- Muscholik, G. Multiple Emulsions for Food Use. *Curr Opin Colloid Interface Sci.* **2007**, 12, 213-220.
- Sawant, A.; Kamath, S.; KG, H.; Kulyadi, G. P. Solid-in-Oil-in-Water Emulsion: An Innovative Paradigm to Improve Drug Stability and Biological Activity. *AAPS PharmSciTech* **2021**, 22, 199.
- Ohwaki, T.; Nitta, K.; Ozawa, H.; Kawashima, Y.; Hino, T.; Takeuchi, H.; Niwa, T. Improvement of the Formation Percentage of Water-in-oil-in-water Multiple Emulsion by the Addition of Surfactants in the Internal Aqueous Phase of the Emulsion. *Int. J. Pharm.* **1992**, 85, 19-28.
- Yun, J. W. Yun; Chung, Y. M. Optimization of Ascorbic Acid Encapsulation in PLA Microcapsules Using Double Emulsion Process. *Appl. Chem. Eng.* **2024**, 35, 115-121.
- Maa, Y. F.; Hsu, C. C. Effect of Primary Emulsions on Microsphere Size and Protein-Loading in the Double Emulsion Process, *J. Microencapsul.* **1997**, 14, 225-241.
- Zhou, J.; Schutzman, R.; Shi, N.-Q.; Ackermann, R.; Olsen, K.; Wang, Y.; Schwendeman, S. P. Influence of Encapsulation Variables on Formation of Leuprolide-loaded PLGA Microspheres. *J. Colloid Interface Sci.* **2023**, 636, 401-412.
- Gander, B.; Merkle, H. P.; Nguyen, V. P.; Ho, N.-T. A New Thermodynamic Model to Predict Protein Encapsulation Efficiency in Poly(lactide) Microspheres. *J. Phys. Chem.* **1995**, 99, 16144-16148.
- Smith, W. R.; Moucka, F.; Nezbeda, I. Osmotic Pressure of Aqueous Electrolyte Solutions via Molecular Simulations of Chemical Potentials: Application to NaCl. *Fluid Phase Equilib.* **2016**, 407, 76-83.

Publisher's Note The Polymer Society of Korea remains neutral with regard to jurisdictional claims in published articles and institutional affiliations.